vibration

MDPI

Article

Ultrasonic Signal Time-Expansion Using DAC Frequency Modulation

Massimiliano Rossi *,† and Marco Frasca †

MBDA Italia S.p.A., Via Monte Flavio, 45, 00131 Rome, Italy; marco.frasca@mbda.it
* Correspondence: massimiliano.rossi@mbda.it
† These authors contributed equally to this work.

Abstract: Ultrasonic signals can be conveniently recorded using modern high-speed analog-to-digital converters and analyzed through digital signal processing algorithms. Sometimes, in some applications, such as in bioacoustics, it is necessary to convert digital data to analog signals with a special transformation that allows compressing and translating the spectrum toward audible frequencies. The process is called time expansion and can be conveniently achieved by slowing down the frequency clock of a digital-to-analog converter. This paper analyzes in detail the spectral characteristics of a time-expanded signal.

Keywords: ultrasound; time-expansion; DAC

check for updates

Citation: Rossi, M.; Frasca, M. Ultrasonic Signal Time-Expansion Using DAC Frequency Modulation. *Vibration* **2023**, *6*, 466–476. https://doi.org/10.3390/vibration6030029

Academic Editors: Jan Awrejcewicz, Junhui Hu and Ming Yang

Received: 23 May 2023
Revised: 14 June 2023
Accepted: 25 June 2023
Published: 27 June 2023

1. Introduction

The time-expansion process of ultrasonic signals allows performing a non-linear transformation in order to compress and translate the spectrum in the audio frequency range, preserving all of the spectral information.

Time expansion is a well-known and widely adopted technique, for example, in bioacoustics and biodiversity-monitoring studies [1–3], where passive sensing is a powerful tool for the detection and classification of species that use ultrasonic sonar pulses for echolocation. Such research requires the collection of audio recordings at ultrasonic frequencies that can reach peaks up to 212 KHz [4] for bat call pulses. To this purpose, bioacoustic research tools consist of dedicated, handheld, and lightweight digital ultrasound recorders that typically operate with sampling frequencies from 200 to 500 KHz. As human ears cannot perceive ultrasounds at all, the biologist performs a local analysis on an audible copy of the original ultrasonic pulses through a lossless time-expansion process provided by the recorder. The device allows storing full-spectrum data or even only the time-expanded version, but both provide an analog time-expanded copy of the signal to the operator. Extensive time and frequency analyses of pulse calls (spectrograms) are often performed in post-processing [5].

Time expansion is a well-known and widely adopted technique, for example, in digital signal audio processing [6–14] where both basic and advanced algorithms are available in order to change the playback speed of a recorded signal and, if needed, preserve the pitch. At times, the available hardware does not have enough computational power to put in place sophisticated algorithms or, more simply, if the output signal has to be in analog form, strictly speaking, fully digital processing may not be required. If the time-expanded signal playback speed reduction v can be written as $v = \frac{N}{M}$ with N and M as integer factors, a digital signal approach will require [13] several operations. Generally, an upsampling process of order M, low-pass filtering with a cut-off frequency of $f_{c_1} = \frac{f_s}{2M}$, a low-pass filtering with a cut-off frequency of $f_{c_2} = \frac{f_s}{2N}$, and a final downsampling of order N are required. Moreover, an analog output signal requires a final analog reconstruction filter. On the other hand, the same task can be successfully accomplished by acting only and directly on the playback frequency of the digital-to-analog section (the DAC frequency modulation). It can be demonstrated that this technique, when conveniently applied, can generate an analog signal whose spectrum results in a compressed and translated copy of the original. Moreover, the DAC frequency modulation technique does not require DSP computational power at all, but it still acts on sampled signals. The process that is beneath such a technique requires clear knowledge of the spectral proprieties of a sampled and time-expanded signal in order to obtain a correct reconstruction.

We do not consider noise in this work; it appears rather interesting to extend these ideas to noisy situations, such as those considered in, e.g., refs. [15,16].

While there is a large amount of literature available for purely numerical techniques, the same is not true, to the authors' knowledge, for the technique discussed here.

The paper is organized as follows: In Section 2, we discuss the mathematical aspects of this technique. In Section 3, we present the experimental results. Finally, in Section 4, we provide a discussion of the main results.

2. Materials and Methods

Experimental evidence is presented through a properly designed ultrasound receiver used for this study.

A proof of the theorem is given in the following sections based on the settings below:

- A sampled sinusoidal ultrasonic signal is time-expanded with the calculation of its spectrum.
- The process is generalized to a generic band-limited signal.

2.1. Sinusoidal Input

Considering an analog input signal of the form

$$x(t) = \cos(2\pi f_o t), \tag{1}$$

and the following definitions:

$$f_s = \frac{1}{T_s} = Sampling\ frequency.$$

$$f_p = \frac{1}{T_p} = Playback\ frequency.$$

$$f_o = \frac{1}{T_o} = Input\ signal\ frequency.$$

$$N = \frac{f_s}{f_p} = Time\ Expansion\ factor.$$

It is assumed that the analog input signal (1) is sampled at a *rate* f_s, respecting the Nyquist criterion. We assume that signal (1) is sampled, and the samples are stored in a suitable memory, to reconstruct it with a digital-to-analog converter (DAC) clocked at a *rate* $f_p \ll f_s$. The resulting output signal can be written as follows:

$$y(t) = \sum_{k=-\infty}^{+\infty} \cos(2\pi f_o k T_s)\,\mathrm{Rect}\left[\frac{t - kT_p}{T_p}\right]. \tag{2}$$

An example of signal (2) is presented in Figure 1, considering a time-expansion factor $N = 20$.

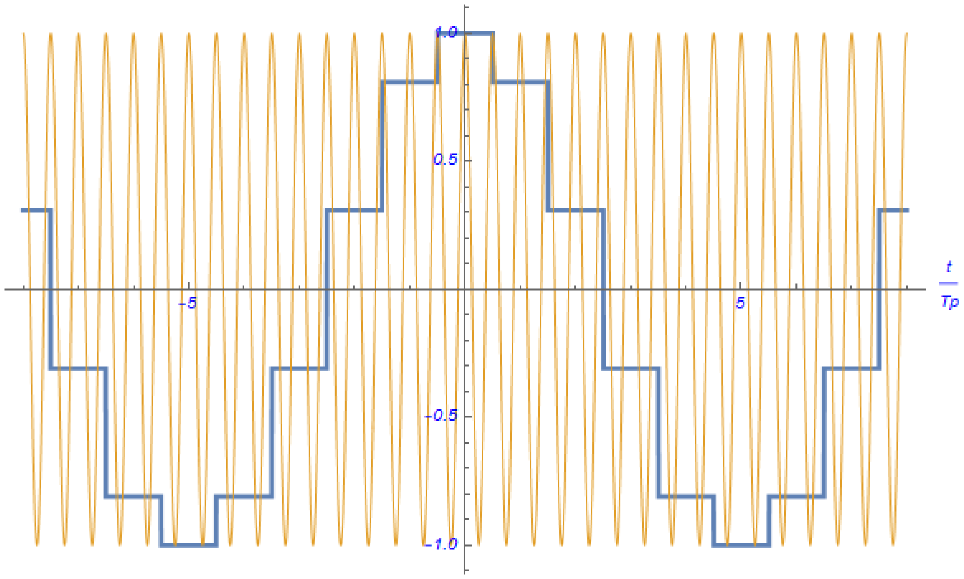

Figure 1. Original (orange) and time–expanded (blue) signals.

The spectrum of the signal $y(t)$ can be put in the form

$$Y(f) = T_p \operatorname{Sinc}(f T_p) \sum_{k=-\infty}^{+\infty} \cos(2\pi f_o k T_s) e^{-i2\pi k T_p} \tag{3}$$

The index k theoretically extends from minus infinity to plus infinity, but it is practically limited to the number of samples effectively recorded. From the symmetry properties of the complex exponential, it is possible to write

$$Y(f) = T_p \operatorname{Sinc}(f T_p) \left(1 + 2\sum_{k=1}^{+\infty} \cos\left(2\pi k f T_p\right) \cos(2\pi f_o k T_s)\right), \tag{4}$$

or, using well-known trigonometric formulas,

$$Y(f) = T_p \operatorname{Sinc}(f T_p) \left(1 + \sum_{k=1}^{+\infty} \cos\left(2\pi k f T_p + 2\pi f_o k T_s\right) + \cos\left(2\pi k f T_p - 2\pi f_o k T_s\right)\right). \tag{5}$$

The instantaneous phases of the cosine terms of (5) are of the form

$$\phi = 2\pi k\left(f T_p \pm f_o T_s\right). \tag{6}$$

The magnitude $|Y(f)|$ exhibits relative maxima at the frequencies, such that

$$\phi = 2\pi k\left(f T_p \pm f_o T_s\right) = 2\pi k n, \tag{7}$$

with $n = 0, \pm 1, \pm 2, \ldots$. So, the key frequencies are

$$f = \frac{1}{N}(n f_s \pm f_o). \tag{8}$$

For $n = 0$, the cosine terms in (5) are in-phase for the same frequency

$$f = \frac{f_o}{N}, \tag{9}$$

generating an absolute maximum exactly at the desired output frequency according to the performed time-expansion process.

2.2. Extension to Passband Ultrasonic Signals

Generalizing, it is possible to consider a real, time-continuous, and band-limited signal $x(t)$ with a bandwidth of B Hz centered around a generic frequency f_o.

We assume sampling of such a signal at a sampling frequency $f_s = \frac{1}{T_s} \geq 2B$ and its reconstruction using a lower frequency $f_p \ll f_s$, with $\frac{f_s}{f_p} = N$, thus having

$$x_c(t) = \sum_{k=-\infty}^{+\infty} x(kT_s)\,\mathrm{Rect}\left[\frac{t-kT_p}{T_p}\right]. \tag{10}$$

The Fourier transform $X_c(f)$ of $x_c(t)$ can be written as

$$X_c(f) = T_p\,\mathrm{Sinc}(f\,T_p) \sum_{k=-\infty}^{+\infty} x(kT_s)e^{-i2\pi kT_p}. \tag{11}$$

Now, it is possible to consider a real signal $y(t) = x\left(\frac{t}{a}\right)$ with $a > 1$, in this case $a = \frac{T_p}{T_s}$. The signal $y(t)$ is a time-expanded copy of $x(t)$.

It is noteworthy to underline that $y(t)|_{t=kT_p} = y(kT_p) = x\left(\frac{T_s}{T_p}\,kT_p\right) = x(kT_s)$, so it is possible to write

$$x_c(t) = \sum_{k=-\infty}^{+\infty} y(kT_p)\,\mathrm{Rect}\left[\frac{t-kT_p}{T_p}\right], \tag{12}$$

from which follows the expression of the Fourier transform

$$X_c(f) = T_p\,\mathrm{Sinc}(f\,T_p) \sum_{k=-\infty}^{+\infty} y(kT_p)e^{-i2\pi kfT_p}. \tag{13}$$

If $Y(f)$ is the Fourier transform of $y(t)$, then from the Poisson summation formula, it follows that

$$T_p \sum_{k=-\infty}^{+\infty} y(kT_p)e^{-i2\pi kfT_p} = \sum_{k=-\infty}^{+\infty} Y\left(f - \frac{k}{T_p}\right). \tag{14}$$

As $y(t)$ is, by definition, the time-expanded signal of $x(t)$, from the properties of the Fourier Transforms [17], it follows that

$$Y(f) = aX(a\,f). \tag{15}$$

The spectrum of $y(t)$ is compressed and scaled by the quantity $a = \frac{T_p}{T_s}$ that is the time-expansion factor.

Thus,

$$T_p \sum_{k=-\infty}^{+\infty} y(kT_p)e^{-i2\pi kT_p} = \sum_{k=-\infty}^{+\infty} Y\left(f - \frac{k}{T_p}\right) = a \sum_{k=-\infty}^{+\infty} X\left(a\,f - \frac{k}{T_s}\right). \tag{16}$$

Finally, it is possible to write

$$X_c(f) = T_p\,\mathrm{Sinc}(f\,T_p) \sum_{k=-\infty}^{+\infty} y(kT_p)e^{-i2\pi kT_p} = \frac{T_p}{T_s}\,\mathrm{Sinc}(f\,T_p) \sum_{k=-\infty}^{+\infty} X\left(a\,f - \frac{k}{T_s}\right). \tag{17}$$

The spectrum of the reconstructed discrete-time signal is formed by compressed and translated replicas, as expected, of $x(t)$. The expected output is centered around the frequency $f = \frac{f_o}{\frac{T_p}{T_s}} = \frac{f_o}{N}$; the first, which is nearest to the origin, is centered around the frequency

$$f_r = \frac{\frac{1}{T_s} - f_o}{\frac{T_p}{T_s}} = \frac{f_s - f_o}{N}. \tag{18}$$

Thus, there is no aliasing if the playback frequency f_p is chosen, respecting the condition $f_p \geq 2\frac{f_o}{N} + \frac{B}{N}$. The signal $x_c(t)$ is frequency-compressed; a suitable ratio $N = \frac{T_p}{T_s}$ is chosen, with a spectrum translated into the audio band, which can be filtered using a low-pass filter with a cut-off frequency,

$$f_{co} = \frac{f_o}{N} + \frac{B}{2N}, \tag{19}$$

in order to reconstruct the analog signal and avoid frequency aliasing.

2.3. Simulations Results

The time-expansion process was simulated using a 100 KHz sinusoidal input signal sampled at 333.3 Ksps using a Matlab script. Assuming a time-expansion factor of $N = 20$, the spectrum of the output signal should be ideally formed only by a spectral content at 5 KHz. The output signal spectrum generated by the model is depicted in Figure 2.

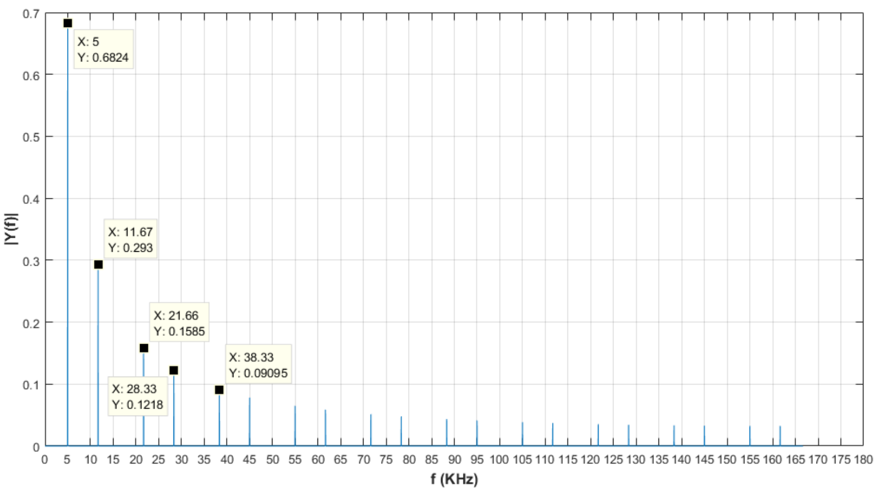

Figure 2. Spectrum of the time-expanded sinusoidal signal.

Where it is clearly visible that the output spectrum is formed by the desired 5 KHz tone plus a series of other spurious tones not harmonically tied with the fundamental. All the spectral components are visible in Figure 2 and result in perfect agreement with (8). The result is summarized in Table 1, where the spurious component order is limited to $n \leq 4$ for better clarity while the desired tone corresponds to $n = 0$.

Table 1. Spectrum of the time-expanded sinusoidal tone.

fo (KHz)	fs (KHz)	n	f_out (KHz)	
100	333.33	0		5
100	333.33	1	11.66	21.66
100	333.33	2	28.33	38.33
100	333.33	3	44.99	54.99
100	333.33	4	61.66	71.66

For the verification of (16), we consider an ultrasonic pulse as the test waveform for the time-expansion process as follows:

$$x(t) = \cos(2\pi f_o t)e^{-\frac{t^2}{2\sigma^2}}. \tag{20}$$

Such a signal is visible in Figure 3 and corresponds to a 200 µs Gaussian pulse oscillating at 100 KHz with a bandwidth of $\frac{1}{\sigma} \simeq 30$ KHz.

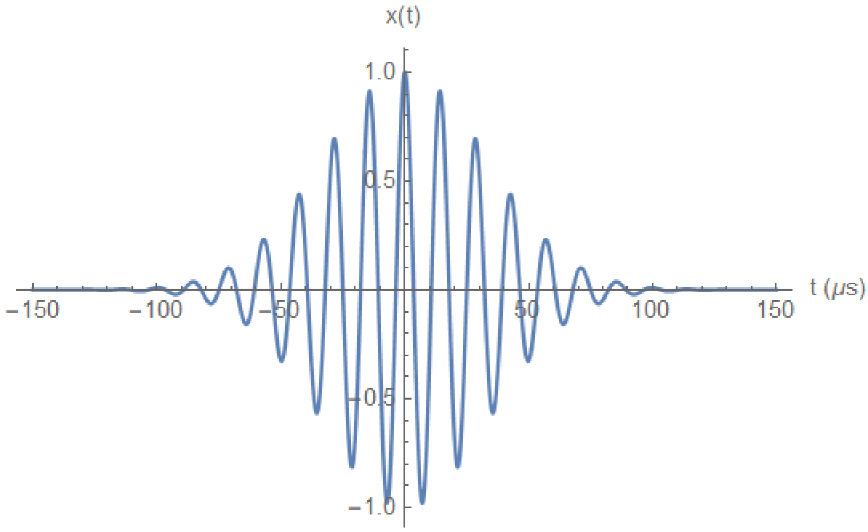

Figure 3. Ultrasonic input pulse.

The Fourier transform of (20) can be written as [17,18]

$$Y(f) = F\{x(t)\} = F\{\cos(2\pi f_o t)\} * F\left\{e^{-\frac{t^2}{2\sigma^2}},\right\} \tag{21}$$

where the symbol * is the convolution operator. So, we can write

$$Y(f) = \left[\frac{1}{2}\delta(f - f_0) + \frac{1}{2}\delta(f + f_0)\right] * \sigma\sqrt{2\pi}e^{-2\pi^2\sigma^2 f^2} \tag{22}$$

$$Y(f) = \frac{\sigma\sqrt{2\pi}}{2}e^{-2\pi^2\sigma^2(f-f_o)^2} + \frac{\sigma\sqrt{2\pi}}{2}e^{-2\pi^2\sigma^2(f+f_o)^2} \tag{23}$$

with $B \simeq \frac{1}{\sigma}$. The magnitude of the spectrum $|Y(f)|$ of the pulse (20) is represented in Figure 4.

The time-expansion process, in this case with a time-expansion factor of $N = 20$, modifies $Y(f)$, generating a spectrum whose magnitude is reported in Figure 5 together with the *Sinc* envelope.

The compressed pulses are centered exactly at the same frequencies calculated with (8) using a sinusoidal input. The signal $y(t)$ is compressed in the frequency by a factor of N and, consequently, time-expanded by the same factor N, so its duration is around four *ms* as clearly visible in Figure 6.

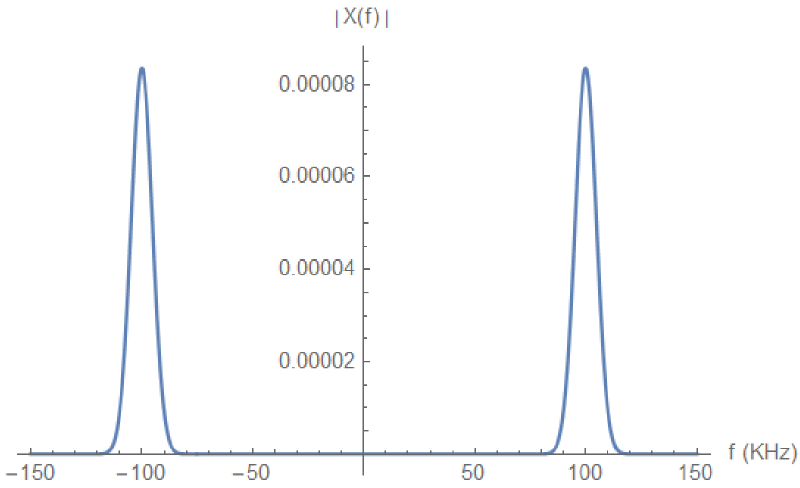

Figure 4. Spectrum of the band-limited signal.

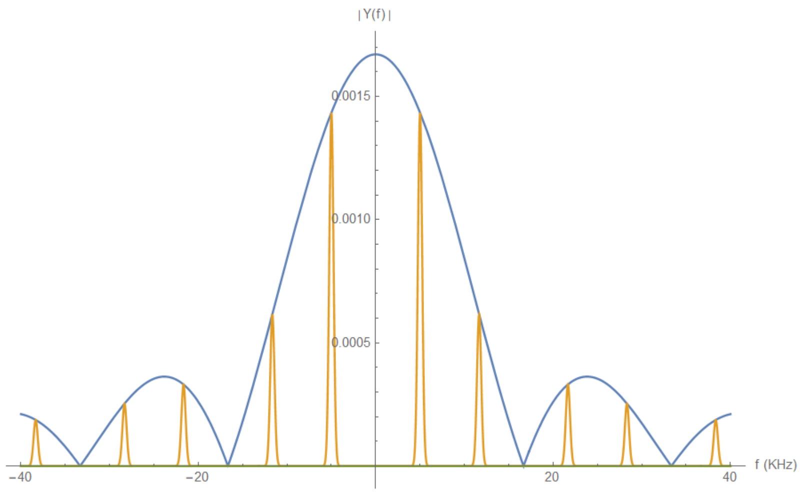

Figure 5. Spectrum of the Time-Expanded of Gaussian ultrasonic pulse (orange) and Sinc Envelope (blue).

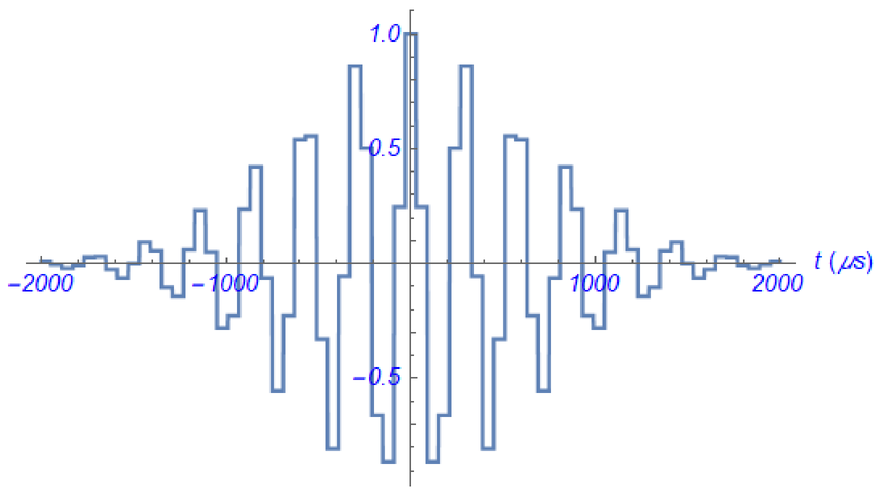

Figure 6. Time-Expanded Gaussian pulse.

3. Experimental Results

In order to confirm the theory, an experimental characterization was conducted with a multi-mode ultrasonic receiver depicted in Figure 7, along with the adopted instrumentation using an input analog sinusoidal signal at 100 KHz, as presented in Figure 8, and then sampled at $f_s = 333.3$ Ksps.

The samples were stored in a high speed 1 MB SRAM and the reconstruction was made at a rate of $f_p = 15.665$ Ksps, 20 times lower than the sampling frequency. The resulting signal in the digital-to-analog converter output is shown in Figure 9.

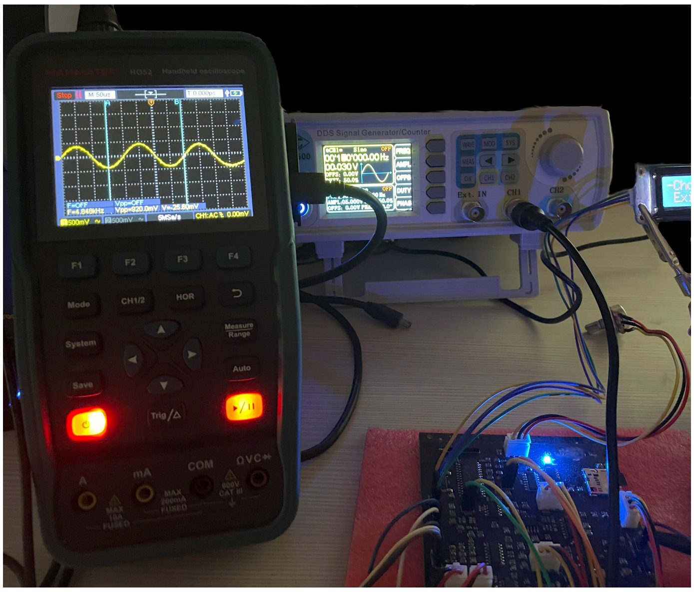

Figure 7. Time–expansion ultrasonic receiver and experimental setup.

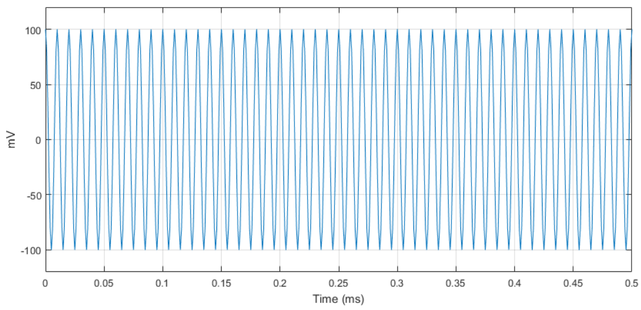

Figure 8. Sinusoidal ultrasonic input test signal.

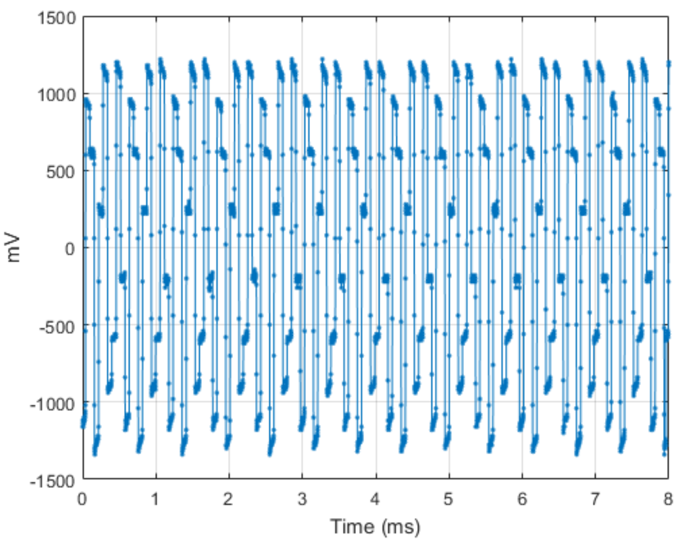

Figure 9. Signal at the DAC output.

The spectrum of the signal of Figure 9 is reported in Figure 10.

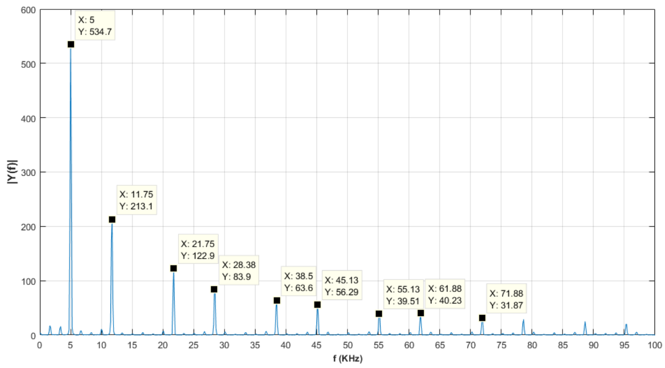

Figure 10. Spectrum of the DAC output signal.

The desired tone and the spurs, reported in Table 2, are in perfect agreement with the theory and with Table 1.

Table 2. Spectrum of the reconstructed time-expanded tone.

fo (KHz)	fs (KHz)	n	f_out (KHz)	
100	333.3	0		5
100	333.3	1	11.7	21.7
100	333.3	2	38.3	45.1
100	333.3	3	55.1	61.8

The discrete-time signal was filtered with a low-pass elliptic filter of order 5, whose cut-off frequency $f_{co} = 6$ KHz was selected according to: (19); the time-expanded analog output signal is presented in Figure 11.

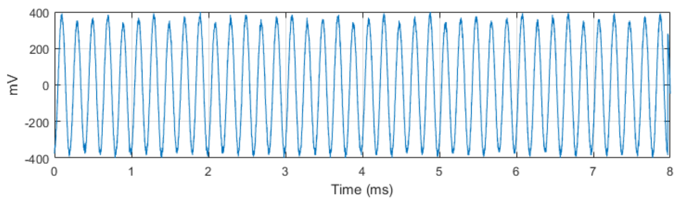

Figure 11. Sinusoidal time-expanded analog output signal.

The perfect reconstruction of the waveform, in the analog domain, is confirmed by its spectrum, as presented in Figure 12.

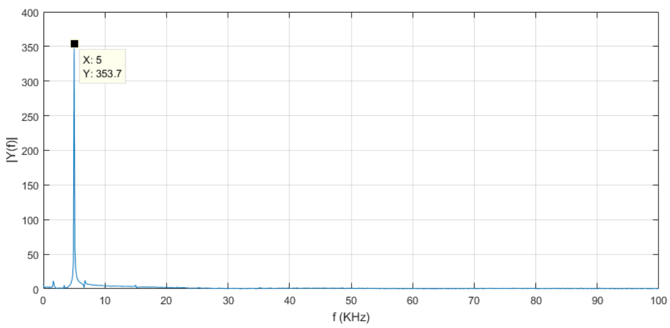

Figure 12. Spectrum of the reconstructed and filtered signal.

4. Discussion

In this paper, the mathematical implications of the time-expansion process of pass-band ultrasonic signals were discussed. The results obtained have general validity and are not intrinsically limited to ultrasonic signals, but the time expansion can be successfully adopted in order to make such signals audible to human ears. In particular, it was emphasized that the spectral properties of these signals are generated by slowing down the DAC playback frequency to f_p Ksps, while dealing with samples collected at a sampling frequency $f_s \gg f_p$ Ksps, ensuring no loss of information. The technique can be considered effective when an analog output signal is required, when the DSP power is not enough to fully put in place digital signal processing algorithms, or when this process is not strictly necessary. Theoretical and experimental results provide detailed images of the spectral properties of the signal from the DAC and allow the designer to define the performance of the reconstruction filter and its cut-off frequency. It is noteworthy that the filter can be an integrated switched capacitor [19], whose cut-off frequency can be easily tuned by just changing its driving clock frequency. This provides an additional degree of freedom to the discussed technique.

Author Contributions: Conceptualization, formal analysis, validation, and software, M.R.; original draft preparation, M.R. and M.F.; review and editing, M.F. All authors have read and agreed to the published version of the manuscript.

Funding: This research received no external funding.

Data Availability Statement: Not applicable.

Conflicts of Interest: The authors declare no conflict of interest.

Abbreviations

The following abbreviations are used in this manuscript:

DAC	digital-to-analog converter
Ksps	kilo samples per second
MDPI	Multidisciplinary Digital Publishing Institute

References

1. Mac Aodha, O.; Gibb, R.; Barlow, K.E.; Browning, E.; Firman, M.; Freeman, R.; Harder, B.; Kinsey, L.; Mead, G.R.; Newson, S.E.; et al. Bat detective—Deep learning tools for bat acoustic signal detection. *PLoS Comput. Biol.* **2018**, *14*, e1005995. [CrossRef] [PubMed]
2. Stathopoulos, V.; Zamora-Gutierrez, V.; Jones, K.E.; Girolami, M. Bat Echolocation Call Identification for Biodiversity Monitoring: A Probabilistic Approach. *J. R. Stat. Soc. Ser. C Appl. Stat.* **2018**, *67*, 165–183. [CrossRef]
3. Russo, D.; Jones, G. Identification of twenty-two bat species (Mammalia: Chiroptera) from Italy by analysis of time-expanded recordings of echolocation calls. *J. Zool.* **2002**, *258*, 91–103 [CrossRef]
4. Thiagavel, J.; Santana, S.E.; Ratcliffe, J.M. Body Size Predicts Echolocation Call Peak Frequency Better than Gape Height in Vespertilionid Bats. *Sci. Rep.* **2017**, *7*, 828. [CrossRef]
5. Fraser, E.E.; Silvis, A.; Brigham, R.M.; Czenze, Z.J. *Bat Echolocation Research: A Handbook for Planning and Conducting Acoustic Studies*, 2nd ed.; Bat Conservation International: Austin, TX, USA, 2020.
6. Zölzer, U. Time-segment processing. In *DAFX: Digital Audio Effects*, 2nd ed.; Helmut Schmidt University—University of the Federal Armed Forces City: Hamburg, Germany, 2011; pp. 185–215.
7. Ferreira, A.J.S. A new frequency domain approach to time-scale expansion of audio signals. In Proceedings of the 1998 IEEE International Conference on Acoustics, Speech and Signal Processing, ICASSP '98 (Cat. No.98CH36181), Seattle, WA, USA, 15 May 1998; Volume 6, pp. 3577–3580. [CrossRef]
8. Laroche, J.; Dolson, M. Improved phase vocoder time-scale modification of audio. *IEEE Trans. Speech Audio Process.* **1999**, *7*, 323–332. [CrossRef]
9. Ferreira, A.J.S. An odd-DFT based approach to time-scale expansion of audio signals. *IEEE Trans. Speech Audio Process.* **1999**, *7*, 441–453. [CrossRef] [PubMed]
10. Dun, Y.; Liu, G. A Fine-Resolution Frequency Estimator in the Odd-DFT Domain. *IEEE Signal Process. Lett.* **2015**, *22*, 2489–2493. [CrossRef]

11. Ferreira, A.J.S. Accurate estimation in the ODFT domain of the frequency, phase and magnitude of stationary sinusoids. In Proceedings of the 2001 IEEE Workshop on the Applications of Signal Processing to Audio and Acoustics (Cat. No.01TH8575), New Platz, NY, USA, 24 October 2001; pp. 47–50.
12. Berthaut, F.; Janin, D.; Martin, B. Advanced Synchronization of Audio or Symbolic Musical Patterns: An Algebraic Approach. *Int. J. Semant. Comput.* **2012**, *6*, 409–427. [CrossRef]
13. Zölzer, U. Time-Frequency Processing. In *DAFX: Digital Audio Effects*; Wiley: Hoboken, NJ, USA, 2011; pp. 219–278. [CrossRef]
14. Almenar, V.; Girona, A.; Flores, S.; Marin-Roig, J. Transmit Diversity Scheme for OFDM Systems Using the Odd DFT. *IEICE Trans. Commun.* **2011**, *E94-B*, 2411. [CrossRef]
15. Stojanovic, V.; Nedic, N. Robust Kalman filtering for nonlinear multivariable stochastic systems in the presence of non-Gaussian noise. *Int. J. Robust Nonlinear Control.* **2016**, *26*, 445–460. [CrossRef]
16. Stojanovic, V.; Nedic, N.; Prsic, D.; Dubonjic, L. Optimal experiment design for identification of ARX models with constrained output in non-Gaussian noise. *Appl. Math. Model.* **2016**, *40*, 6676–6689. [CrossRef]
17. Marks, R.J. *Handbook of Fourier Analysis & Its Applications*; Oxford University Press: Oxford, UK, 2009. [CrossRef]
18. Kahrs, M.; Brandenburg, K. *Applications of Digital Signal Processing to Audio and Acoustics*; Springer: Berlin/Heidelberg, Germany, 2013.
19. Winder, S. *Analog and Digital Filter Design*; Elsevier: Amsterdam, The Netherlands, 2002.